ISSN 0975-6299 Vol 2/Issue 1/ Jan-Mar 2011

International Journal of Pharma and Bio Sciences

REVIEW ARTICLE

PHARMACEUTICS

MICRONEEDLES: PROMISING TECHNIQUE FOR TRANSDERMAL DRUG DELIVERY.

Corresponding Author

JAYDEEP D YADAV

Department of Pharmaceutical Sciences, N.D.M.V.P. Samaj's, College of Pharmacy, Gangapur Road, Nasik- 422 002, Maharashtra, India.

Co Authors

KUMAR A VAIDYA, PRIYANKA R KULKARNI and RAJVAIBHAV A RAUT.

Department of Pharmaceutical Sciences, N.D.M.V.P. Samaj's, College of Pharmacy, Gangapur Road, Nasik- 422 002, Maharashtra, India.

ABSTRACT

Transdermal drug delivery using microneedle is a novel method of drug delivery. Microneedle is like conventional needles only fabricated in micro scale. The advantage of using microneedle is that it does not pass the stratum corneum. The dosing in microgram quantities can be done by this type of needle. The mechanism of action is based on temporary mechanical disruption of skin. The drug, in the form of biomolecules, is encapsulated within the microneedles, which are then inserted into the skin in the same way a drug like nitroglycerine is released into the bloodstream from a patch. The needles dissolve within minutes, releasing the trapped cargo at the intended delivery site. The review covers the various methods of drug delivery like Poke with patch approach, Coat and poke approach, Biodegradable microneedles, Hollow microneedles and Dip and scrape. The various method of preparation of microneedles include molding, casting, laser cutting. The in vivo safety assessment and the evaluation of microneedle have shown that this technique can be used safely. There are various advantages of the microneedle trans dermal drug delivery methods over other techniques which helps to make it successful delivery system.

KEYWORDS

Trandermal drug delivery, Microneedle, polydimethyl siloxane,

INTRODUCTION

Microneedle, a microstructured transdermal system, consists of an array of microstructured projections coated with a drug or vaccine that is applied to the skin to provide intradermal delivery of active agents, which otherwise would not cross the stratum corneum.[1]

Microneedles are somewhat like traditional needles, but are fabricated on the micro scale. They are generally one micron in diameter and range from 1-100 microns in length. Microneedles have been fabricated with various materials such as: metals, silicon, silicon dioxide, polymers, glass and other materials. It is smaller then hypodermic needle, the less it hurts when it pierces skin and offer several advantages when compared to conventional needle technologies. The major advantage of microneedles over traditional needles is, when it is inserted into the skin it does not pass the stratum corneum, which is the outer 10-15 µm of the skin. Conventional needles which do pass this layer of skin may effectively transmit the drug but may lead to infection and pain. As for microneedles they can be fabricated to be long enough to penetrate the stratum corneum, but short enough not to puncture nerve endings. Thus reduces the chances of pain, infection, or injury.[2]

Various types of needles have been fabricated as well, for example: solid (straight, bent, filtered), and hollow. Solid microneedles could eventually be used with drug patches to increase diffusion rates; solid-increase permeability by poking holes in skin, rub drug over area, or coat needles with drug. Hollow needles could eventually be used with drug patches and timed pumps to deliver drugs at specific times. Arrays of hollow needles could be used to continuously carry drugs into the body using simple diffusion or a pump system. Hollow microneedles could also be used to remove fluid from the body for analysis – such as blood glucose measurements – and to then supply microliter volumes of insulin or other drug as required. The hollow needle designs include tapered and beveled tips, and could eventually be used to deliver microliter quantities of drugs to very specific locations. The researchers demonstrated that an array of 400 microneedles can be used to pierce human skin delivering drug macromolecules. Very small microneedles could provide highly targeted drug administration to individual cells. These are capable of very accurate dosing, complex release patterns, local delivery and biological drug stability enhancement by storing in a micro volume that can be precisely controlled.[3]

ADVANTAGES OF MICRONEEDLES

1. The major advantage of microneedles over traditional needles is, when it is inserted into the skin it does bypass the stratum corneum, which is the outer 10-15 µm of the skin. Conventional needles which do pass this layer of skin may effectively transmit the drug but may lead to infection and pain. As for microneedles they can be fabricated to be long enough to penetrate the stratum corneum, but short enough not to puncture nerve endings. Thus reduces the chances of pain, infection, or injury.[4]
2. By fabricating these needles on a silicon substrate because of their small size, thousands of needles can be fabricated on single water. This leads to high accuracy, good reproducibility, and a moderate fabrication cost.
3. Hollow like hypodermic needle; solid— increase permeability by poking holes in

skin, rub drug over area, or coat needles with drug

4. Arrays of hollow needles could be used to continuously carry drugs into the body using simple diffusion or a pump system.
5. Hollow microneedles could be used to remove fluid from the body for analysis – such as blood glucose measurements – and to then supply microliter volumes of insulin or other drug as required.[5]
6. Immunization programs in developing countries, or mass vaccination or administration of antidotes in bioterrorism incidents, could be applied with minimal medical training.
7. Very small microneedles could provide highly targeted drug administration to individual cells.
8. These are capable of very accurate dosing, complex release patterns, local delivery and biological drug stability enhancement by storing in a micro volume that can be precisely controlled.

NEED FOR USING MICRONEEDLES

When oral administration of drugs is not feasible due to poor drug absorption or enzymatic degradation in the gastrointestinal tract or liver, injection using a painful hypodermic needle is the most common alternative. An approach that is more appealing to patients, and offers the possibility of controlled release over time, is drug delivery across the skin using a patch. However, transdermal delivery is severely limited by the inability of the large majority of drugs to cross skin at therapeutic rates due to the great barrier imposed by skin's outer stratum corneum layer.[6]

To increase skin permeability, a number of different approaches has been studied, ranging from chemical/lipid enhancers[7] to electric fields employing iontophoresis and electroporation to pressure waves generated by ultrasound or photoacoustic effects. Although the mechanisms are all different, these methods share the common goal to disrupt stratum corneum structure in order to create “holes” big enough for molecules to pass through. The size of disruptions generated by each of these methods is believed to be of nanometer dimensions, which is large enough to permit transport of small drugs and, in some cases, macromolecules, but probably small enough to prevent causing damage of clinical significance.[8]

An alternative approach involves creating larger transport pathways of microns dimensions using arrays of microscopic needles. These pathways are orders of magnitude bigger than molecular dimensions and, therefore, should readily permit transport of macromolecules, as well as possibly supramolecular complexes and microparticles. Despite their very large size relative to drug dimensions, on a clinical length scale they remain small. Although safety studies need to be performed, it is proposed that micron-scale holes in the skin are likely to be safe, given that they are smaller than holes made by hypodermic needles or minor skin abrasions encountered in daily life .[9]

Transdermal drug delivery is a non-invasive, user-friendly delivery method for therapeutics. However, its clinical use has found limited application due to the remarkable barrier properties of the outermost layer of skin, the stratum corneum (SC). Physical and chemical methods have been developed to overcome this barrier and enhance the transdermal delivery of drugs. One of such techniques was the use of microneedles to temporarily compromise the skin barrier layer. This method combines the advantages of conventional injection needles and transdermal patches while minimizing their disadvantages. As compared to hypodermic needle injection, microneedles can provide a minimally invasive means of painless delivery of therapeutic molecules through the skin barrier with precision and convenience. The microneedles seldom cause infection while they can allow drugs or nanoparticles to permeate through the skin. Increased microneedle-assisted transdermal delivery has been demonstrated

for a variety of compounds. For instance, the flux of small compounds like calcein, diclofenac methyl nicotinate was increased by microneedle arrays. In addition, microneedles also have been tested to increase the flux of permeation for large compounds like fluorescein isothiocynate-labeled Dextran, bovine serum albumin, insulin and plasmid DNA and nanospheres.

Microneedles may create microconduits sufficiently large to deliver drug-loaded liposomes into the skin. The combination of elastic liposomes and microneedles may provide higher and more stable transdermal delivery rates of drugs without the constraints of traditional diffusion-based transdermal devices, such as molecular size and solubility. Though it could offer benefits mentioned above, the combined use of elastic liposomes and microneedle pretreatment has received little attention.

MECHANISM OF ACTION

The mechanism for delivery is not based on diffusion as it is in other trandsermal drug delivery products. Instead, it is based on the temporary mechanical disruption of the skin and the placement of the drug or vaccine within the epidermis, where it can more readily reach its site of action.

The drug, in the form of biomolecules, is encapsulated within the microneedles, which are then inserted into the skin in the same way a drug like nitroglycerine is released into the bloodstream from a patch. The needles dissolve within minutes, releasing the trapped cargo at the intended delivery site. They do not need to be removed and no dangerous or biohazardous substance is left behind on the skin, as the needles are made of a biodegradable substance.

In microneedle devices, a small area (the size of a traditional transdermal patch) is covered by hundreds of microneedles that pierce only the *stratum corneum* (the uppermost 50 µm of the skin), thus allowing the drug to bypass this important barrier (Figure 1). The tiny needles are constructed in arrays to deliver sufficient amount of drug to the patient for the desired therapeutic response.[10]

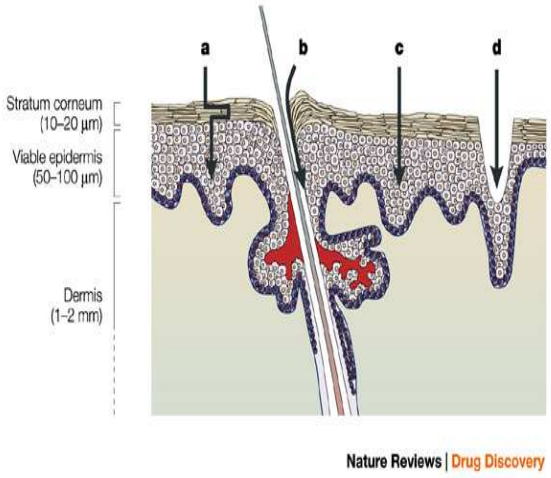

Figure 1
Delivery site for microneedle technology.

METHODOLOGY OF DRUG DELIVERY[11]

A number of delivery strategies have been employed to use the microneedles for transdermal drug delivery.

These include

- Poke with patch approach
- Coat and poke approach
- Biodegradable microneedles
- Hollow microneedles
- Dip and scrape

Poke with patch approach

It involves piercing an array of solid microneedles into the skin followed by application of the drug patch at the treated site. Transport of drug across skin can occur by diffusion or possibly by iontophoresis if an electric field is applied.

Coat and poke approach

In this approach needles are first coated with the drug and then inserted into the skin for drug release by dissolution. The entire drug to be delivered is coated on the needle itself.

Biodegradable microneedles

It involves encapsulating the drug within the biodegradable, polymeric microneedles, followed by the insertion into the skin for a controlled drug release.

Hollow microneedles

It involves injecting the drug through the needle with a hollow bore. This approach is more reminiscent (suggestive of) of an injection than a patch.

Dip and scrape

Dip and scrape approach, where microneedles are first dipped into a drug solution and then scraped across the skin surface to leave behind the drug within the microabrasions created by the needles. The arrays were dipped into a solution of drug and scraped multiple times across the skin of mice in vivo to create microabrasions. Unlike microneedles used previously, this study used blunt-tipped microneedles measuring 50–200 μm in length over a 1 cm^2 area.

PREPARATION OF MICRONEEDLES

General method of microneedle preparation[12]

Molding

Micromolds were fabricated using photolithography and molding processes. In brief, a female microneedle master-mold was structured in SU-8 photoresist by UV exposure to create conical (circular cross section) or pyramidal (square cross section) microneedles tapering from a base measuring 300 μm to a tip measuring 25 μm in width over a microneedle length of 600–800 μm. A male microneedle master-structure made of polydimethylsiloxane was created using this mold. The PDMS master-structure was sputter-coated with 100 nm of gold to prevent adhesion with a second PDMS layer cured onto the male master-structure to create a female PDMS replicate-mold. Excess PDMS on the female replicate-mold was trimmed so that the mold fit within the 27-mm inner diameter of a 50 ml conical tube. This metal-coated male master-structure was repeatedly used to make replicate-molds that were repeatedly used to make microneedle devices.

Preparation of microneedle matrix

To serve as microneedle matrix materials, ultra-low viscosity carboxymethylcellulose (CMC), amylopectin and bovine serum albumin (BSA) were dissolved in deionized water. Water was then evaporated off until the concentration of solute (e.g., CMC) was approximately 27 wt%, which resulted in a viscous hydrogel. CMC was concentrated by heating at 60–70 °C at ambient pressure or vacuuming at −50 kPa at room temperature. Amylopectin and BSA were concentrated only by the heating method at 60–70 °C or 37 °C, respectively. Solute concentration was determined by measuring solution mass before and after evaporation. Viscosity of concentrated hydrogels was measured using a Couette viscometer.

In some cases, a model drug was added by hand mixing to solubilize or suspend the

compound in the concentrated hydrogel. Three model drugs were added at final concentrations of 0.15–30 wt% sulforhodamine B (Molecular Probes), 20 wt% BSA (Sigma), or 5 wt% lysozyme (Sigma). The term "model drug" is used to indicate that these compounds have physicochemical and transport properties representative of certain classes of drugs, but not to suggest that these compounds have pharmacological activity representative of drugs.

Casting

To mold microneedles from concentrated hydrogels, 100–300 mg of hydrogel was placed on a female PDMS mold in a conical centrifuge tube (Corning) and centrifuged in a 45° angled rotor at 3000 × g and 37 °C for up to 2 h to fill the microneedle mold cavities and dry the hydrogel. To prepare microneedles with model drug encapsulated only within the microneedles and not in the backing layer, 8–10 mg of hydrogel mixed with model drug was filled just into the microneedle cavities in the mold and then dried under centrifugation for up to 30 min. Residual hydrogel on the surface of the mold was removed with dry tissue paper and 100–200 mg pure hydrogel without drug was then applied and dried onto the mold to form the backing layer. To prepare microneedles with model drug encapsulated only in the backing layer and not within the microneedles, the same 2-step process was followed, except pure hydrogel was filled into the microneedle mold cavities and a hydrogel mixed with model drug was used to form the backing layer.

Other methods[10]

Laser cutting

Microneedles were cut from stainless steel sheets using an infrared laser. The desired microneedle shape and dimensions were first drafted in AutoCAD software. Using this design, the infrared laser was operated at 1000 Hz, 20 J/cm^2 energy density and 40% attenuation of laser energy to cut the microneedles. A total of three passes were required to completely cut through the stainless steel sheet. A cutting speed of 2 mm/s and air purge at a constant pressure of 140 kPa was used. Microneedles were either prepared as individual rows of needles ('in-plane' needles) or as two-dimensional arrays of needles cut into the plane of the stainless steel sheet and subsequently bent at 90° out of the plane ('out-of-plane' needles).

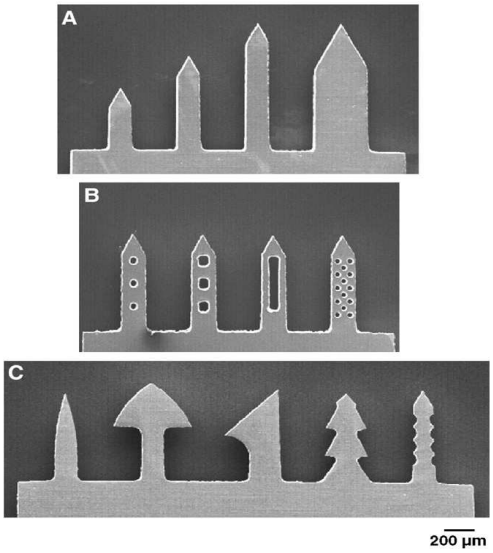

Fig.2
Different shapes of microneedles

Cleaning and bending microneedles

Laser-cut stainless steel microneedle arrays were manually cleaned with detergent to de-grease the surface and remove slag and oxides deposited during laser cutting, which was followed by thorough rinsing in running water. To prepare 'out-of-plane' microneedles, microneedles cut into stainless steel sheets were first manually pushed out of the sheet using either forceps or a hypodermic needle (26 gage, 1/2 inch long) while viewing under a stereo microscope, and then bent at 90° angle with the aid of a #9 single-edged razor blade.

Electropolishing

To clean microneedle edges and to make the tips sharp, microneedles were electropolished in a solution containing glycerin, ortho-phosphoric acid (85%) and water in a ratio of 6:3:1 by volume. Electropolishing was performed in a 300 ml glass beaker at 70 °C and a stirring rate of 150 rpm. A copper plate was used as the cathode, while microneedles acted as the anode. The anode was vibrated at a frequency of 10 Hz throughout the electropolishing process using a custom-built vibrating device to help remove gas bubbles generated at the anodic surface during electropolishing. A current density of 1.8 mA/mm^2 was applied for 15 min to electropolish the microneedles. After electropolishing, microneedles were cleaned by dipping alternately three times in de-ionized water and 25% nitric acid for 30 s each. This was followed by another washing step in hot running water and a final wash in running de-ionized water. Due to the electropolishing process, the thickness of the microneedles was reduced to 50 µm. Microneedles were dried using compressed air before storing in air-tight containers until later use.

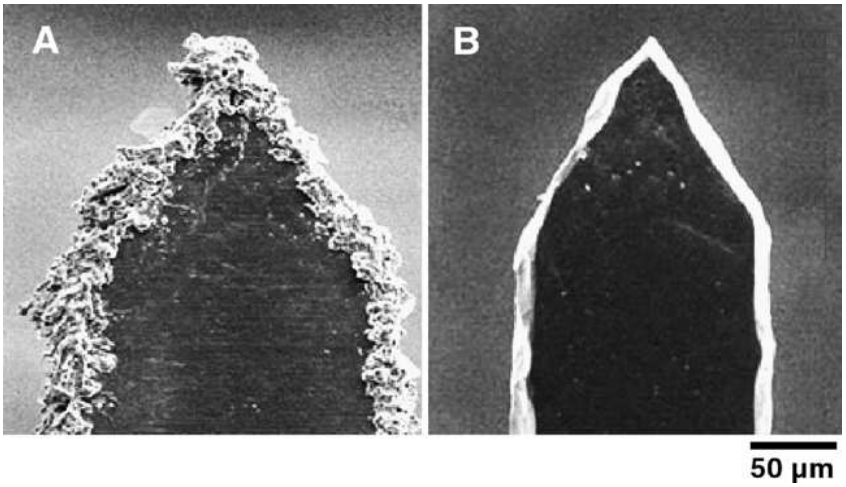

Fig.3

Effect of electropolishing on microneedle surface. Scanning electron micrographs of: (A) a microneedle tip with slag and debris residue remaining after cleaning with detergent powder and (B) a microneedle tip after electropolishing, resulting in removal of slag and debris, clean edges, and sharp tip.

Micro-dip-coating

Microneedles were coated with different molecules using a novel micron-scale, dip-coating process and a specially formulated coating solution.

a. *Coating solution*

The coating solution was composed of 1% (w/v) carboxymethylcellulose sodium salt (low viscosity, USP grade), 0.5% (w/v) Lutrol F-68 NF and a model drug/biopharmaceutical. The model drugs tested included 0.01% suforhodamine, 0.01% calcein, 3% vitamin B , 1% bovine serum albumin conjugated to Texas Red (Molecular Probes), 0.05% gWiz™ luciferase plasmid DNA, 2×10^9 plaque forming units per ml of modified vaccinia virus-Ankara, 10% barium sulfate particles (1 μm diameter), 1.2% 10-μm diameter latex beads and 8.2% 20-μm diameter latex beads, all w/v. DNA and virus were made fluorescent by incubating with YOYO-1 (Molecular Probes) at a dye: base pair/virus ratio of 1:5 for 1 h at room temperature in the dark.

b. ***Coating single microneedles***

Single microneedles were dip-coated by horizontally dipping the microneedle into 20–30 μl of coating solution held as a droplet on the tip of a 200-μl large-orifice pipette tip. The large-orifice pipette tip was mounted horizontally in a clamp and the microneedle was mounted opposite to it on a manual linear micropositioner. Immersion withdrawal of the microneedle into the liquid droplet was performed manually by moving the microneedle while viewing under a stereo microscope.

c. ***Coating rows of microneedles***

In-plane rows of microneedles were dip-coated using an in-house designed coating device. The coating device consisted of two parts:

(1) The coating-solution reservoir and (2) the micropositioning dip coater.

(1) ***Coating-solution reservoir***

The coating-solution reservoir was designed to restrict access of the coating liquid only to the microneedle shaft to prevent contamination of the base. The coating-solution reservoir consisted of two laminated parts: the 'bottom plate' and the 'cover plate', both of which were made of polymethylmethacrylate (Fig. 4A). The bottom plate had a central feeding channel (1 mm deep × 0.5 mm wide) machined into one of its faces, with a through-hole drilled across to the other face. This hole acted as the inlet port to fill the channel with the coating solution. The cover plate had five holes (400 μm diameter) drilled into it at the same interval as the microneedles in the in-plane row to be coated. These 'dip-holes' acted as individual dipping reservoirs to coat each of the microneedles in the row. The two plates (bottom and cover plates) were aligned and adhered to each other using solvent bonding with methylene chloride (Fisher Scientific) as the solvent.

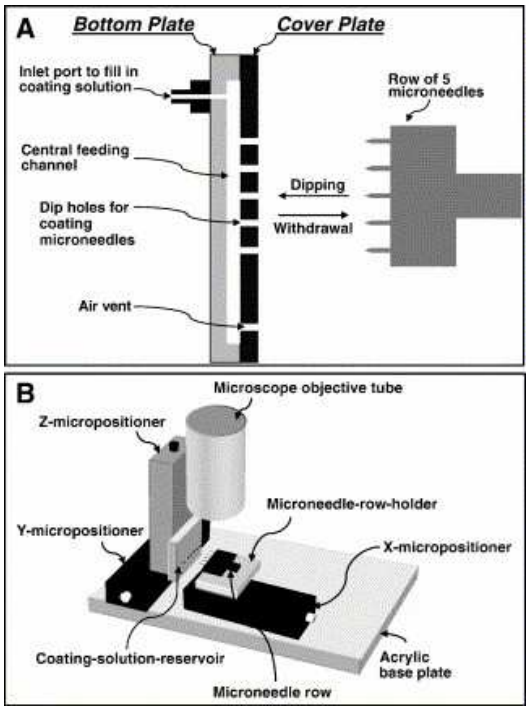

Fig.4

Schematic diagrams of in-plane microneedle row-coating device. (A) Cross sectional view of the coating-solution reservoir showing the microneedles aligned with the dip-holes. (B) Isometric projection of the entire device showing the X, Y and Z-micropositioners used to align the microneedles with dip-holes of the coating-solution reservoir. The cylindrical tube represents the stereo-microscope objective, which is used to view the microneedle alignment and coating process facilitating manual control.

(2) *Micropositioning dip coater*

To enable three-dimensional alignment and dipping of microneedle rows into the dip-holes, three linear-micropositioners were assembled on a 6.35-mm thick, flat, acrylic plate (Fig. 4B). The first micropositioner was used to control the position of the in-plane microneedle row. The other two micropositioners were assembled one on top of the other on the acrylic plate to create a composite Y–Z motion micropositioner that was used to control the position of the coating-solution reservoir. The three micropositioners together allowed the alignment of the in-plane microneedle row to the dip-holes. The X-micropositioner was used to horizontally dip the microneedles into and out of the dip-holes. The coating was performed manually while viewing under a stereo microscope. Control over the length of the microneedle shaft to be coated was exercised manually using the X-micropositioner. Tolerance for misalignment was included by designing the dip-hole diameter to be twice the width of the microneedles.

BIODEGRADABLE POLYMER MICRONEEDLE FABRICATION PROCESSES[13]

The process to fabricate biodegradable polymer microneedle is based on micromolding using high-aspect-ratio SU-8 epoxy photoresist or polyurethane master structures to form PDMS (polydimethyl siloxane) molds from which biodegradable polymer microneedle replicates are formed.

Beveled-tip master structures

Microneedles with beveled tips were fabricated by first creating a master structure from SU-8 epoxy using ultraviolet (UV) lithography (Fig. 5). SU-8 epoxy with photoinitiator was coated to a thickness of 300–350 μm onto a silicon wafer and lithographically patterned into 100 μm diameter cylinders, which defined the shape of the desired needles. Although these cylinders were usually circular in cross-section, sometimes a different mask was used to create cylinders with a notch of 30-μm radius cut out of one side. These cylinders were arranged in an array, where the center-to-center spacing between cylinders in each row was 1400 μm and between each column was 400 μm. The array contained 20 cylinders in each row arranged in 6 columns for a total of 120 cylinders in an area of 9 × 9 mm.

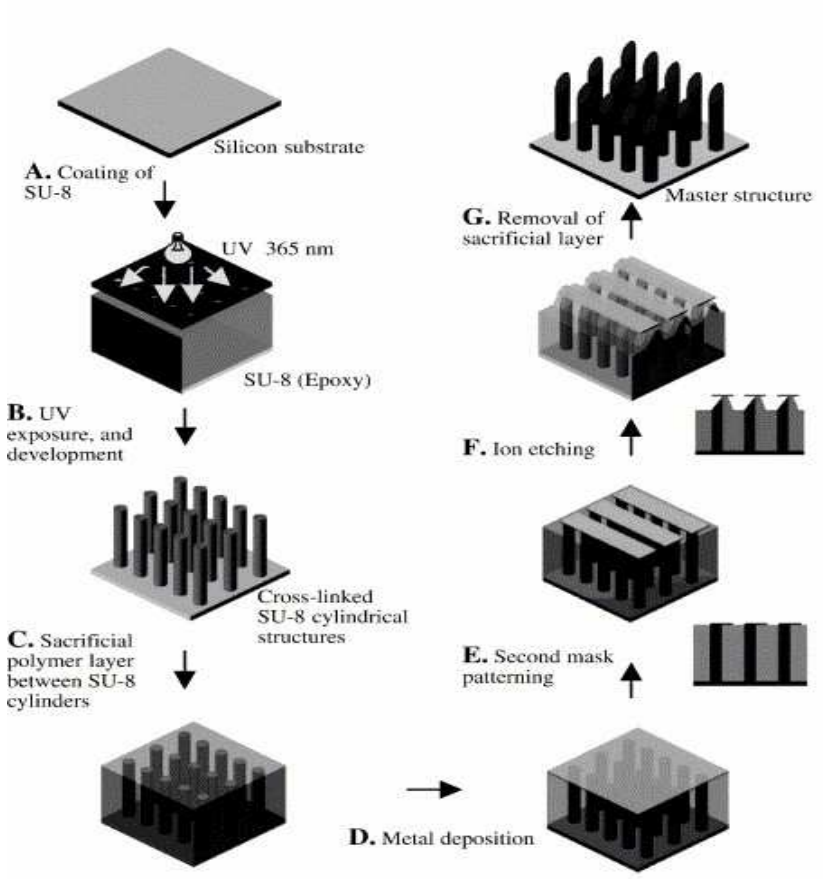

Fig.5

Schematic of process to fabricate beveled-tip microneedle SU-8 photoresist is lithographically defined and developed to yield an array of cylinders.

After filling the spaces between cylinders with a sacrificial polymer and lithographically placing a metal mask asymmetrically on top of each row of cylinders, the cylinders are ion etched to produce an array of microneedle with beveled tips to be used as a master structure for subsequent molding.The space between cylinders was filled with a sacrificial polymer and the entire surface was coated with a 600-nm thick layer of copper by electron beam.This copper layer was etched with acid (H_2SO_4 : H_2O_2 : H_2O at a volumetric ratio of 1 : 1 : 10) to leave a pattern of rectangles with 0.6 mm width and 10 mm length that asymmetrically covered the tops of the epoxy cylinders and some of the sacrificial polymer on one side of each cylinder. Reactive

ion partially removed the uncovered sacrificial layer and asymmetrically etched the tip of the adjacent epoxy cylinders. All remaining sacrificial polymer was removed by ethyl acetate, leaving an array of epoxy cylinders with asymmetrically beveled tips.

Chisel-tip master structures

Chisel-tip microneedles were fabricated using a combination of wet silicon etching and reactive ion etching of polymers (Fig.6). Silicon nitride was deposited onto a silicon wafer to a thickness of 4000 Å by chemical vapor deposition to make a hard mask to protect silicon against KOH etching. Next, the silicon nitride layer was lithographically patterned to expose a 15 × 15 array of square dots each measuring 100 µm in width with 600-µm center-to-center spacing. The exposed silicon nitride layer was removed using reactive ion etching and the photoresist was then removed using acetone. KOH heated to 80 °C was then applied to the wafer to etch inverted pyramid-shaped holes. Etching occurred along the crystal plane to form 55°-tapered walls terminating in a sharp point, which provide the chisel shape of the needle tips.

To form the shape of the needle shaft, SU-8 epoxy photoresist with photoinitiator was spin-coated onto the etched wafer to form a 500-µm thick film. A second mask was aligned with the wafer to expose the SU-8 coating to UV light in the same 15 × 15 array of square dots in vertical alignment with the silicon nitride pattern. After post-baking to crosslink the UV-exposed SU-8 on a hotplate for 30 min at 100 °C and then cooling, the non-crosslinked epoxy was developed with PGMEA to leave behind obelisk-shaped SU-8 structures with their tips still embedded in the silicon wafer.

To finally make master needle structures, the space between the obelisk structures was filled with PDMS. The crosslinked SU-8 was removed by reactive ion etching with oxygen plasma to leave a PDMS-silicon mold. Subsequently, polyurethane was poured into the mold and crosslinked to form polymeric microneedle with chisel tips. Removal of these needles from the mold yielded the final master structure

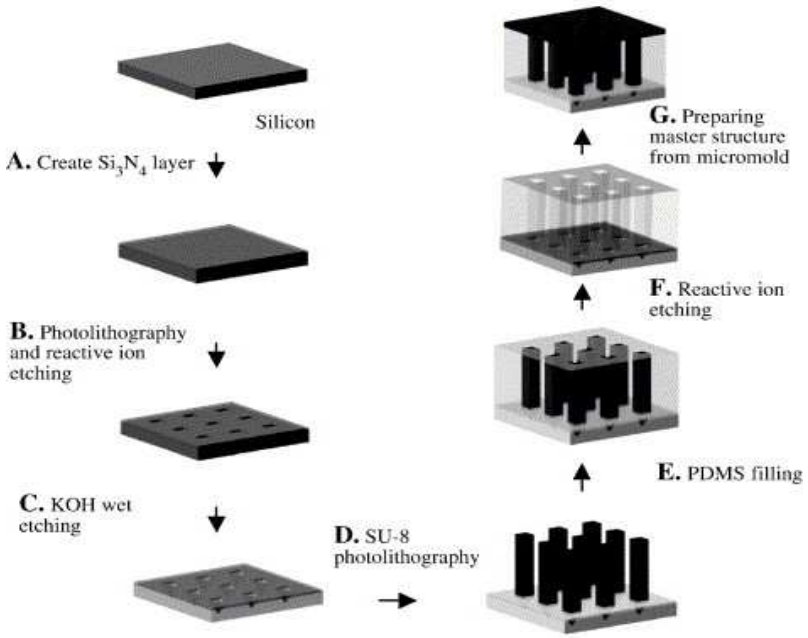

Fig.6
Schematic of process to fabricate chisel-tip microneedle

Using a lithographically defined Si_3N_4 mask, inverted pyramids are wet-etched into a <1,0,0> silicon substrate. SU-8 photoresist is lithographically patterned into each pyramid hole and as square columns on top. After surrounding the array of SU-8 structures with PDMS and removing SU-8 by reactive ion etching, the resulting mold is used to form an array of chisel-tip out of polyurethane to be used as a master structure for subsequent molding

Tapered-cone master structures

Tapered-cone microneedle were fabricated using a novel lens-based technique (Fig.7). A 5300 Å thick, opaque chromium layer was sputter-deposited and lithographically patterned on a glass substrate (sodalime glass) for form a 20 × 10 array of circular dots each measuring 100 μm in diameter with 400 μm center-to-center spacing. Glass etchant (HF: HCl: H_2O at a volumetric ratio of 1: 2: 17) was used to isotropically etch the glass substrate through the openings in the patterned chromium layer to create concave holes in the glass of 70 μm radius/depth. Casting of SU-8 photoresist with photoinitiator created a 1000- or 1500-μm thick film on the substrate with bumps that filled the concave holes.

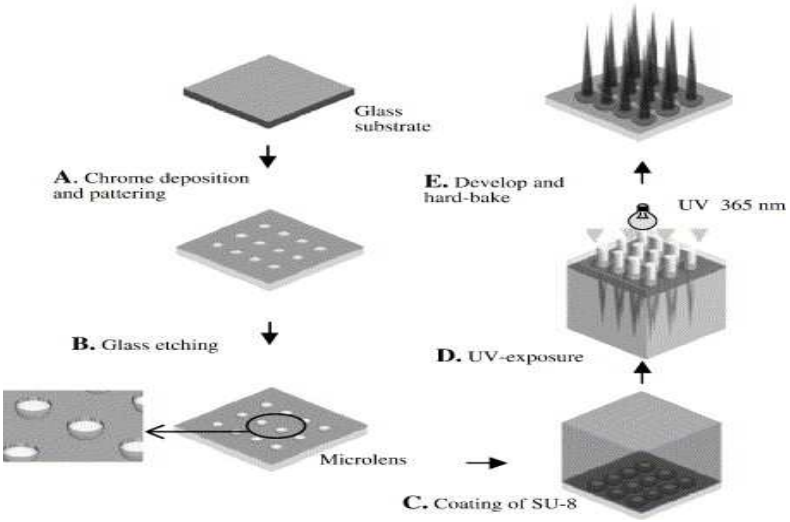

Fig.7

Schematic of integrated lens process to fabricate tapered-cone microneedle

Using a lithographically defined metal mask, a glass substrate is wet-etched to produce an array of hemispherical invaginations that form microlenses. After filling and covering these invaginations with a thick layer of SU-8 photoresist, UV light is shined through the glass substrate, forming latent images in the SU-8 layer that define the shape of an array of tapered-cone microneedle produced after development that are used as a master structure for subsequent molding.

After soft-baking (100 °C, 12 h), the film was exposed from the bottom (through the glass substrate) to UV light. Due to the refractive index difference between the glass substrate and SU-8 resist, the bumps formed integrated microlenses. Light was blocked from passing through the areas between the microlenses due to the opaque chromium layer. Light shining through the lenses was focused within the SU-8 film to give latent images in the shape of tapered cones with a base diameter equal to the

circular dot diameter of the chromium mask (i.e., 100 µm) and a length of, for example, 1000 µm, as determined by microlens geometry. Subsequent development of the unexposed SU-8 left a master structure of tapered-cone microneedle.

IN VIVO ASSESSMENT OF SAFETY OF MICRONEEDLE ARRAYS IN HUMAN SKIN[14]

Microneedle skin insertion

To determine if microneedles insert into skin, CMC pyramidal microneedles (600 µm height, 300 µm base width, and 600 µm center-to-center spacing) in a 10 × 10 array were inserted with IACUC approval into full-thickness cadaver pig skin without subcutaneous fat that was shaved and affixed under mild tension to a wooden plate using 1 cm long screws. Microneedles were inserted by pressing against the microneedle backing layer with a thumb using a force of approximately 1.5 N and then removed immediately after the insertion. The site of microneedle insertion on the skin surface was exposed for 10 min to a red tissue-marking dye (Shandon, Pittsburgh, PA, USA) that selectively stains sites of stratum corneum perforation. After wiping residual dye from the skin surface with dry tissue paper, skin was viewed by brightfield microscopy. Skin samples were prepared for histology by freezing in histology mounting compound and slicing into 20-µm thick sections and then viewed by brightfield microscopy.

Barrier function

The TEWL values after treatment with the 200S, 300S and 400S are provided in Fig.8a. Prior to treatment, TEWL values were around 9.5 g h^{-1} m^{-2}. The 200S treatment did not result in increased TEWL values and 15 min after piercing the TEWL values only decreased and reached values that were below the initial baseline values. After piercing with the 300S, TEWL values increased immediately and declined after 15 min reaching baseline values after 30 min. The pattern of the TEWL values obtained after treatment with the 400S was similar to that obtained with the 300S, but the effect lasted 15 min longer. Treatment with the microneedle arrays showed a trend that longer microneedles result in a higher increase in TEWL values. Only a significant difference in response was observed between the 400S and 200S (Table 1). In Fig.8b the increase in TEWL after treatment with microneedles of different shapes, positive control (550A), negative control (550A) and two-fold application is provided. In this study all treatments were compared to the treatment with the 300S microneedle arrays. For almost all microneedle arrays the TEWL values increased and reached a peak directly after application. After the first time point at 0 min the TEWL decreased very slowly, but did not return to the baseline value within the time frame of the experiment. The 300A was the only treatment that reached its maximum TEWL[15] values not directly after piercing, but 15 min later. TEWL did not increase after treatment with the control. As shown in (Table 2), treatment with the 300S did not increase the TEWL to a significantly higher level than after the control treatment. The highest TEWL values (maximum of 11.8 g h^{-1} m^{-2}) were obtained with the 550A ($P < 0.001$ in comparison to the 300S). Furthermore, the 300A resulted in a significant higher increase in TEWL than the solid microneedle array of the same length ($P < 0.001$) and piercing twice with the 300S microneedle array increased the TEWL significantly compared to a single 300S microneedle treatment ($P < 0.001$).

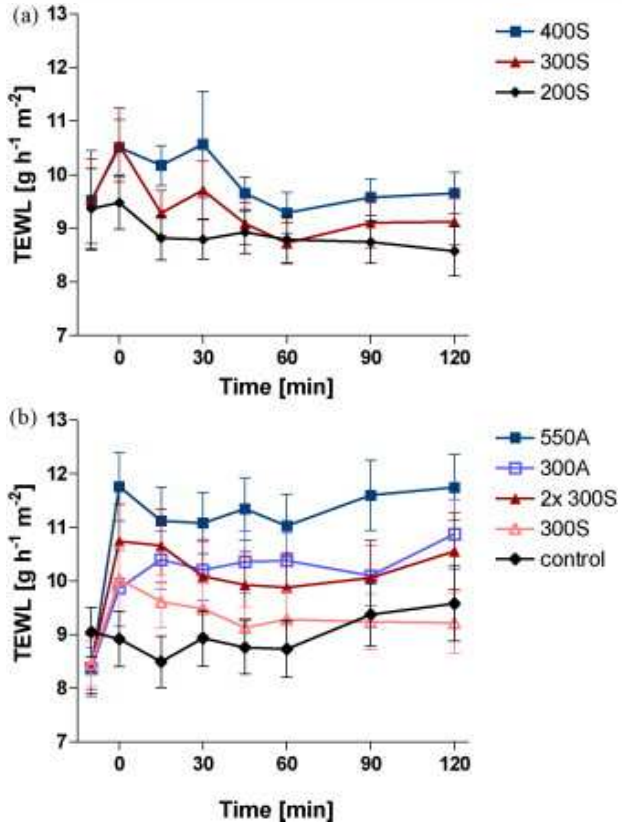

Fig.8
TEWL values before and after applying different microneedle arrays.

The microneedle arrays are applied at t = 0 min. A: assembled hollow metal microneedle arrays; S: solid metal microneedle arrays; control: application of the mould only; 2×: two-fold application. (A) Solid metal microneedle arrays of 200, 300 and 400 µm needle length. The 200S treatment did not result in increased TEWL, the 300S and 400S did. (B) Solid metal microneedle arrays of 300 µm in comparison to different types of microneedle arrays. After application of all microneedle arrays an increase in TEWL was observed. The assembled microneedle arrays induced higher TEWL values than the solid microneedles. Data are presented as average values ± S.E.M. of 18 (A) or 15 (B) volunteers.

TEWL	400S vs 300S	400S vs 200S	300S vs 200S
Mean difference	0.548	1.04	0.495
95% CI	0.149–0.947	0.644–1.44	0.0962–0.894
p value	$p < 0.01$	$p < 0.001$	$p > 0.05$

Table1

Pairwise comparison of TEWL values (g h^{-1} m^{-2}) between solid microneedle arrays of different lengths

TEWL	300S vs 300A	300S vs 2× 300S	300S vs blank	300S vs 550A
Mean difference	−0.884	−0.844	0.458	−1.95
95% CI	−1.33 to −0.435	−1.29 to −0.395	0.00961–0.907	−2.40 to −1.51
p value	$p < 0.001$	$p < 0.001$	$p < 0.05$	$p < 0.001$

In Fig.9a and b box-and-whisker plots of the pain scores as reported by the volunteers are shown. The pain scores of all treatments are similar and very low. No significant differences in pain caused by microneedles of different length or shape were found. The median value of all microneedle arrays was 1, except for the 550A were the median was 2. This array also had the highest maximum pain score of 6. Even though the scores after microneedle treatment and control did not differ significantly, the latter did have the smallest interquartile range.

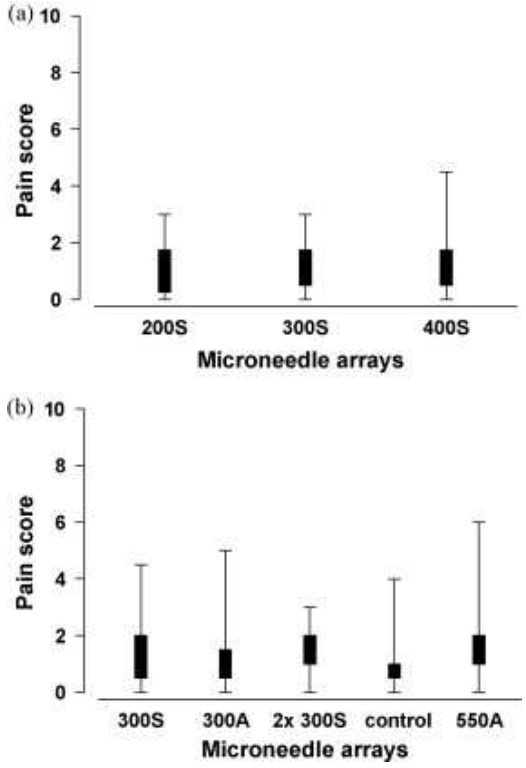

Fig.9

Box-and-whisker plots of the pain scores after treatment with different microneedle arrays.

A: assembled hollow metal microneedle arrays; S: solid metal microneedle arrays; control: application of the mould only; 2×: two-fold application. (A) The median values of all solid microneedles were comparable, but the range of the 400S pain scores is larger. $n = 18$. (B) Treatment with the microneedle arrays resulted in similar pain scores. The interquartile range of the control is smaller than that of the microneedle arrays and more variation in pain scores was observed with the 500A. $n = 15$.

Skin irritation

As a determinant of the degree of irritation the redness of the skin and the blood flow was examined Fig.10a shows the change in redness (Δa) for the solid microneedle arrays of different length. After application of each microneedle array an increase in Δa was observed. After 15 min the Δa values were maximal and reached values of 1.8 absorption units (AU) for the 300S and 400S and of 1.4 AU for the 200S could be detected. From this time on the Δa values decreased and reached baseline values for the 200S after 60 min and for the 300S and 400S after 90 min. As shown in (Table 3) treatment with the 400S resulted in significant higher Δa values than treatment with the 200S ($P < 0.001$). In Fig.10b the Δa after treatment with the 300S was compared to different types of microneedle arrays. Treatment with the empty mould resulted in maximum values directly after application and almost immediately afterwards the baseline values were reached. For all microneedle arrays, the Δa values were maximal 15 min after application, and remained elevated for at least 90 min. Treatment with the 550A and the 300S resulted in Δa values that were still higher after 2 h than before treatment. As shown in (Table 4), treatment with the 300S resulted in an increase that was significantly higher than after the control treatment ($P < 0.001$). After treatment with the 550A, similar Δa levels were reached as with the 300S, while significantly lower values compared to the 300S were found after treatment with the 300A ($P < 0.01$), even though after treatment with the 300A very small spots of blood redness were observed in the skin. Piercing with the 550A also resulted in small blood spots in the skin. Single and two-fold piercing with the 300S microneedle array did not result in significant differences in Δa values.

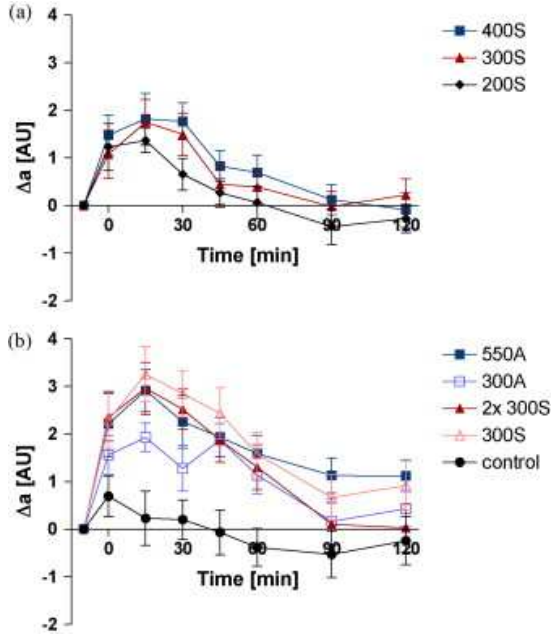

Fig.10

The change in redness (Δ*a*) at different time points after the application of microneedle arrays in comparison to the redness before application. The microneedle arrays are applied at *t* = 0 min. A: assembled hollow metal microneedle arrays; S: solid metal microneedle arrays; control: application of the mould only; 2×: two-fold application. (a) Solid metal microneedle arrays of 200, 300 and 400 µm needle length. Treatment with all microneedle arrays resulted in an increase in Δ*a*. The highest values were obtained with the 400S. (b) Solid metal microneedle arrays of 300 µm in comparison to different types of microneedle arrays. An increase in Δ*a* was observed after treatment with all microneedle arrays, while the control treatment did not result in higher Δ*a* values. Treatment with solid microneedle arrays increased the Δ*a* more than the assembled microneedle arrays. Data are presented as average values ± S.E.M. of 18 (a) or 15 (b) volunteers.

Δ*a*	**400S vs 300S**	**400S vs 200S**	**300S vs 200S**
Mean difference	0.181	0.537	0.356
95% CI	−0.112 to 0.481	0.237 to 0.837	0.0559 to 0.656
p value	$p > 0.05$	$p < 0.001$	$p < 0.05$

Table3

Pairwise comparison of induced redness (AU) between solid microneedle arrays of different lengths

Δ*a*	**300S vs 300A**	**300S vs 2× 300S**	**300S vs blank**	**300S vs 550A**
Mean difference	0.804	0.408	2.01	0.119
95% CI	0.244 to 1.36	−0.152 to 0.967	1.45 to 2.57	−0.441 to 0.679
p value	$p < 0.01$	$p > 0.05$	$p < 0.001$	$p > 0.05$

Table 4

Pairwise comparisons of induced redness (AU) between different types of microneedle arrays

Monitoring changes in subcutaneous blood flow using the LDI were another way to assess skin irritation. In Fig. 5 examples of pictures and perfusion images of skin reactions after five different applications of microneedle arrays are shown. The figure shows scans of the same skin area before treatment and at different time points after treatment. The change in blood flow compared to the baseline values after application of the 200S, 300S and 400S was derived from the blood flow images and is shown in Fig 6a. Immediately after treatment the blood flow increased, but reduced to baseline values within 45 min. However, no

significant differences in blood flow were found after treatment with 400S, 300S and 200S microneedles (Table 5). As shown in Fig. 6b pressing an empty mould against the skin resulted in a slight increase the subcutaneous blood flow, as an increase of 25 PU could be observed, but after 30 min the baseline value was reached again. Applying the microneedle arrays resulted in an immediate increase in blood flow followed by a rapid decrease. The 300S resulted in a significantly higher increase in blood flow than after treatment with the control ($p < 0.001$). The blood flow returned to baseline values within 60 min for all microneedle arrays except the 550A, which values remained elevated for at least 2 h. Treatment with the solid microneedle arrays resulted in a trend of a more pronounced blood flow increase than after applying the assembled microneedles (Table 6). Two-fold and single piercing of 300S microneedle arrays did not result in significant differences in blood flow

ΔBlood flow	400S vs 300S	400S vs 200S	300S vs 200S
Mean difference	19.25	18.82	−0.432
95% CI	−0.177 to 38.68	−0.608 to 38.25	−19.86 to 19.00
p value	$p > 0.05$	$p > 0.05$	$p > 0.05$

Table 5

Pairwise comparisons of the increase in blood flow (PU) between solid microneedle arrays of different lengths

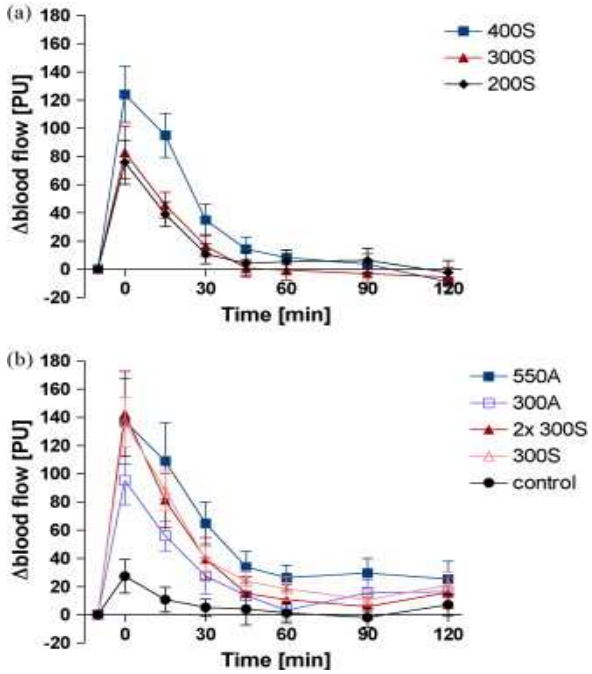

Fig.12

The change in blood flow at different time points after the application of microneedle arrays in comparison to the blood flow before application. The microneedle arrays are applied at *t* = 0 min. A: assembled hollow metal microneedle arrays; S: solid metal microneedle arrays; control: application of the mould only; 2×: two-fold application. (a) Solid metal microneedle arrays of 200, 300 and 400 µm needle length. Treatment with all microneedle arrays resulted in increased blood flow values, but the 400S increased the blood flow the most. (b) Solid metal microneedle arrays of 300 µm in comparison to different types of microneedle arrays. Treatment with all microneedle arrays resulted in increased blood flow values in comparison to the control. Treatment with the solid microneedle arrays increased the blood flow more than the assembled microneedle arrays. Data are presented as average values ± S.E.M. of 18 (a) or 15 (b) volunteers.

ΔBlood flow	**300S vs 300A**	**300S vs 2× 300S**	**300S vs blank**	**300S vs 550A**
Mean difference	15.79	3.823	40.57	−12.6
95% CI	−9.646 to 41.22	−21.61 to 29.26	15.14 to 66.01	−38.04 to 12.83
p value	$p > 0.05$	$p > 0.05$	$p < 0.001$	$p > 0.05$

Table 6
Pairwise comparisons of the increase in blood flow (PU) between different types of microneedle arrays

Skin permeability measurement

To measure changes in skin permeability after treatment with microneedles, we used standard protocols from the transdermal drug delivery literature adapted to microneedles studies. Briefly, heat-stripped epidermis from human cadavers was used because the stratum corneum (i.e., the upper layer of the epidermis) provides the primary barrier to transdermal transport as well as the main mechanical barrier to needle insertion. After the epidermis was placed on ten layers of tissue paper to provide a tissue-like mechanical support, a 5 × 20 array of beveled-tip, PGA microneedles was pierced into the epidermis using a force of 4 N, left in place for 3 s, and removed. The epidermis was then placed onto a support mesh (300 µm polypropylene woven screen cloth) and loaded into a Franz diffusion chamber, which was immersed in a 37 °C water bath containing magnetic stirrers. The lower, receptor compartment was filled with 5 ml of well-stirred phosphate buffer saline in contact with the underside of the viable epidermis. The exposed skin area was 1.8 cm^2. The upper, donor compartment in contact with the stratum corneum was initially filled with PBS for 5 h to permit skin hydration, after which it was filled with 2 ml of either 1 mM calcein or 1 mM fluorescein-conjugated bovine serum albumin in PBS. One hour later, 1 ml of receptor solution was sampled and fluorescence intensity was measured using calibrated spectrofluorometry. Skin permeability was calculated assuming steady state transport across skin.

EVALUATION OF MICRONEEDLES

Imaging and histology

Fluorescence micrographs of coated microneedles and histological skin sections were collected using an Olympus IX70 fluorescent microscope with a CCD camera. Bright field micrographs were collected using an Olympus SZX12 stereo microscope with a CCD camera. Digital X-ray imaging to detect barium sulfate was done using the Faxitron MX20 cabinet X-ray. Histological examination of cadaver skin was conducted on frozen sections. Porcine cadaver skin was pierced with microneedles for 1 min, frozen in OCT compound, and cut into 10-µm thick sections using a cryostat.

In vitro dissolution time and delivery efficiency

Single microneedles (n = 3) coated with vitamin B, calcein or sulforhodamine were inserted into porcine cadaver skin for 10 s or 20 s. Upon removal, these microneedles were imaged by fluorescence microscopy to check for presence of residual coating. To determine the delivery efficiency of coated microneedles, rows of five microneedles coated with vitamin B were inserted into pig cadaver skin for 5 min (n = 3). The mass of vitamin B on the inserted and non-inserted microneedle rows was determined by dissolving the coatings in de-ionized water through vigorous mixing, quantifying the vitamin B concentration in the resulting solution via fluorescence spectroscopy, and multiplying the measured concentration by the volume of de-ionized water used for dissolution to yield the amount of vitamin B that was adherent to the microneedles. Similarly, the mass of vitamin B left behind on the skin surface during microneedle insertion was estimated by applying tape to the skin surface, removing the tape, dissolving the material removed by the tape in de-ionized water, and determining the vitamin B content by fluorescence spectroscopy. Using a mass balance, the amount of vitamin B delivered into the skin was determined by subtracting the amount remaining on the microneedles and on the skin surface after insertion from the amount originally on non-inserted microneedles.

DELIVERY OF MOLECULES AND PARTICLES

Delivery from individual microneedles in vitro

Single microneedles (n = 3) coated with calcein were inserted into porcine cadaver skin for 20 s and removed. For particle delivery, barium sulfate particles (1 µm diameter, as determined by scanning electron microscopy, data not shown), or latex beads (10 or 20 µm diameter) were inserted into porcine cadaver skin for 1 min (n = 3 single microneedles for each insertion). After removing the microneedles, the skin surface was examined by brightfield microscopy for coating residue. Porcine cadaver skin was then examined histologically to assess the extent of delivery of microneedle coatings into the skin. The use of porcine cadaver skin was approved by the Georgia Institute of Technology Institutional Animal Care and Use Committee (IACUC).

Delivery for assembled microneedle patches in vitro and in vivo

For in vitro testing, out-of-plane microneedle arrays (n = 3) were coated, assembled into patches and manually inserted into human cadaver skin for 1 min. After 1 min, the patch was removed and visually examined by brightfield microscopy to qualitatively assess the amount of residual coating left on the microneedles. The human cadaver skin was also imaged by brightfield microscopy to assess release and delivery of coatings into the skin. For in vivo analysis, non-coated patches of out-of-plane arrays were sterilized using ethylene oxide and manually applied onto the forearms of human subjects (n = 3) for 30 s. Gentian violet (a violet topical antifungal agent, 2% solution) was then applied on the treated site for 1 min and wiped away using isopropanol swabs. Gentian violet selectively stained the sites of skin perforation, which identified the sites of microneedle insertion.

The use of human subjects was approved by the Georgia Institute of Technology Institutional Review Board (IRB).

APPLICATIONS OF MICRONEEDLE TECHNOLOGY

Microneedle technology has been developed as a platform technology for delivery of high molecular weight and hydrophilic compounds through the skin. The first ever study of transdermal drug delivery by microarray technology was conducted by Henry *et al* who demonstrated an increase in the permeability of skin to a model compound calcein using microarray technology. In a follow up study, Mc-Allister *et al* found a change in the permeability of cadaver skin to insulin, latex nanoparticles and bovine serum albumin after treatment with microneedles, and unleashed the mechanism of transport as simple diffusion.

Oligonucleotide delivery

Lin and coworkers extended the *in vitro* findings of microarray drug delivery to *in vivo* environment. An oligonucleotide, 20-merphosphorothioated oligodeoxynucleotide was delivered across the skin of hairless guinea pig either alone or in combination with iontophoresis. Lin and coworkers used solid microneedles etched from stainless steel or titanium sheet prepared with the poke with patch approach. This delivery system increased the absorption of the molecules relative to the intact skin. Iontophoresis combined with microneedles was able to increase the transdermal flux by 100 fold compared to the iontophoresis alone.

DNA vaccine delivery[11]

The cells of Langerhans present in the skin serve as the first level of immune defense of the body to the pathogens invading from the environment. These cells locate the antigens from the pathogens and present them to Tlymphocytes, which in turn stimulate the production of antibodies. Mikszta *et a*l reported the delivery of a DNA vaccine using microneedle technology prepared with the dip and scrape approach. The arrays were dipped into a solution of DNA and scrapped multiple times across the skin of mice *in vivo.* Expression of luciferase reporter gene was increased by 2800 fold using microenhancer arrays. In addition, microneedle delivery induced immune responses were stronger and less variable compared to that induced by the hypodermic injections. Similar results were obtained by researchers at Beckett- Dickinson™ in an animal study for antibody response to HepB naked plasmid DNA vaccine 3. This approach has a potential to lower the doses and the number of boosters needed for immunization.

Desmopressin delivery[11]

M. Cormier *et a*l (Alza Corporation, USA) examined the use of microneedles to deliver desmopressin, a potent peptide hormone used in the treatment of nocturnal enuresis in young children, as well as for the treatment of diabetes insipidus and haemophilia A. Microneedles were coated by an aqueous film coating of desmopressin acetate on titanium microneedles of length 200 µm, a maximal width of 170 µm and a thickness of 35 µm. Microneedle patch was inserted into the skin with the help of an impact applicator. A target dose of 20 µg of desmopressin was delivered to hairless guinea pig from 2 cm2 microneedle array within 15 minutes.

Insulin delivery[11]

Insulin is one of the most challenging drug of all times for the drug delivery technologists. Martano *et* al10, used microarrays for the delivery of insulin to diabetic hairless rats. Solid microneedles of stainless steel having 1mm length and tip width of 75 µm were inserted into the rat skin and delivered insulin using poke with patch approach. Over a period of 4 hours, blood glucose level steadily decreased by as much as 80% with the decrease in glucose level being dependent on the insulin concentration.

Porphyrin Precursor 5-Aminolevulinic Acid (ALA) Delivery[11]

Photodynamic therapy of deep or nodular skin tumours is currently limited by the poor tissue penetration of the porphyrin precursor 5-aminolevulinic acid (ALA). Ryan F. Donnelly and co workers have shown that, *in vivo* experiments using nude mice showed that microneedle puncture could reduce application time and ALA dose required to induce high levels of the photosensitiser protoporphyrin IX in skin. This clearly has implications for clinical practice, as shorter application times would mean improved patient and clinician convenience and also that more patients could be treated in the same session.

In vitro transdermal delivery of monoclonal antibody

In all the previously mentioned studies, purified human IgG was used as a model drug for large proteins in transdermal delivery, and later the feasibility of microneedle-mediated transdermal delivery was further investigated using a human monoclonal antibody IgG to demonstrate the applicability of this technique for delivery of macromolecules.

COMMERCIAL MICRONEEDLE TECHNOLOGIES

A decade after the first microneedles were reported, many commercial technologies have come into the market including the Macroflux technology, h-patch, Micro-Trans and many more (Table 7).

Sr. No.	Name of the technology	Manufacturer	Available drug products	Drug products in development
1.	Macroflux	Alza	None	PTH patch, Vaccines, Proteins
2.	h-patch	Valeritas	Bolus insulin delivery	-
3.	Microinfusor	BD	None	Vaccines, Macromolecules
4.	Micro-Trans	Valeritas	None	Fluid sensing of glucose, hormones, blood gases, Vaccines, Proteins
5.	Microstructured transdermal system	3M	None	Hydrophilic molecules, Macromolecules
6.	Micropiles	Texmac-Nanodes	10% Lidocaine and Indomethacin	-
7.	Micro Needle Therapy System	Clinical resolution lab	Microneedle Dermaroller	-

Table7

List of the technology used with the manufacture and the drug products.

Macroflux® transdermal technology

Macroflux technology (Macroflux® Corporation Inc.) expands the scope of microarray technology to a broader group of drugs, from synthetic drugs to therapeutic proteins as well as vaccines. The technology can be drug coated for direct administration or can be used in combination with iontophoresis. The technique employs a thin titanium screen with microprojections of precise dimensions. These microarrays can be dip or dry coated, wherein the dry coating may be utilized for bolus/continuous drug delivery.

Currently the technique is tested for parathyroid hormone delivery by Zosano pharma and is presently in phase 2 clinical trials for treatment of osteoporosis. The technique promises a stable and convenient product for older men and women who are currently using daily injections, thereby providing a hope for improving the patient compliance.

Macroflux® patch and applicator

FUTURE TRENDS

Integration of solid microneedles with transdermal patch provides a minimal invasive method to increase the skin permeability of drugs, including the macromolecules such as proteins. Till date, microneedles made up of silicon, metal, glass and plastics have been utilized for transdermal delivery.[16] However, with rapid advancement in technology, microneedles composed of biodegradable and biocompatible materials have been explored. For instance, fabrication of dissolving microneedles using polysaccharide biomaterials have been utilized for controlled drug delivery. Microneedle approach of drug delivery is currently being evaluated for a number of drugs, but extensive studies would be required to foster the application of these delivery modes in the clinical set up.

Results from several groups suggest that microneedles are a promising, possibly powerful technology for the administration of therapeutics (e.g. vaccines or drugs) into the skin. However, a few issues will have to be studied in greater depth before microneedles can be widely used clinically. Firstly, other methods of improving microneedle penetration (e.g. various ways of limiting the viscoelasticity the skin, coating the needles, further improving needle/array design) should be explored. While high-speed injectors are currently being used, another method may be more feasible especially if the microneedles are integrated into a drug delivery device. Also, microneedles

have been touted as being particularly suited for administration of drugs requiring slow release. Hence, another issue that will need to be looked into is whether the microneedles will remain in the skin (after insertion) and how to keep needles in the skin during normal daily activities.

Several new and interesting microneedle concepts have been recently proposed which may find great utility in the future. For example, biodegradable polymer microneedles have recently been fabricated and characterized. The advantage of polymer needles is that they may be produced much more inexpensively (compared to silicon) and they should not pose a problem if they break in the skin since they are biodegradable. Yet other groups are working on needles which are made of materials that incorporate drugs which are released when the needles dissolve (personal communication).

As the variety of microneedles increases, a comprehensive series of tests that can be applied to test all needles should be proposed. These tests should include pre-clinical tests (in vivo tests in animal models), clinical tests (to test pain, inflammation, etc.), mechanical tests (to evaluate parameters such as margin of safety) as well as fluidic flow tests (e.g. fluid pressure needed for particular flow rate, etc.). This will help not only in objectively comparing the microneedles but aid in the selection of the most appropriate microneedle for each application.

CONCLUSION

Microchannel based Transdermal Delivery System by using Microneedles is a Novel Approach for Drug delivery system. It is a convenient, painless, and less invasive alternative to injection & it can be used a common method for administering large proteins and peptides, antibiotics, vacines in low manufacturing cost. In contrast to oral delivery, microneedles avoid first pass effect and offer the benefit of immediate cessation of drug administration in case of an adverse effect or overdose. In contrast to passive delivery, this allow for the delivery of water-soluble drugs. In contrast to Iontophoresis, this is use for long time. There is also no molecular size limitation, no molecular electrical charge requirement, and no specific formulation pH constraint. In contrast to conventional TDDS, this is use for potent & less potent the drug, the more extended release the delivery system.

REFERENCE

1. S. Henry, D. McAllister, M.G. Allen and M.R. Prausnitz, Microfabricated microneedles. J. Pharm. Sci. 87**,** 922–925, (1998)
2. S. Hashmi, P. Ling, G. Hashmi, M. Reed, R. Gaugler and W. Trimmer, Genetic transformation of nematodes using arrays of micromechanical piercing structures. BioTechniques 19, pp. 766–770, (1995)
3. S.Kaushik, A.H.Hord, S.Smitra, M.R. Prausnitz, Lack of pain associated with microfabricated microneedles. Anesth. Analg. 92 **,** pp. 502–504, (2001)
4. V.P. Shah, Transdermal Drug Delivery, 2nd edition, Marcel Dekker Inc., New York, pp. 365, (2003).
5. D.V. McAllister, O.M. Wang, S.P. Davis, J.K. Park, P.J. Canatella, M.G. Allen and M.R. Prausnitz, Microfabricated needles for transdermal delivery of macromolecules and nanoparticles: Fabrication methods and transport studies Proc. Natl. Acad. Sci. 100(24), 13755–13760, (2003).
6. R.L. Bronaugh and H.I. Maibach, Percutaneous Absorption: Drugs–Cosmetics-Mechanisms-Methodology,

Marcel Dekker, New York, pp. 778-787, (1999).
7. B. Barry and A. Williams, Penetration enhancers. Advanced. Drug Delivery Reviews. 56(5), 603–618, (2004).
8. V. Preat and R. Vanbever, Skin electroporation for transdermal and topical delivery. Adv. Drug Deliv. Rev. 56, 659–674, (2004).
9. R.H. Champion, J.L. Burton, D.A. Burns and S.M. Breathnach, Textbook of Dermatology, Blackwell Science, London, pp. 546-557, (1998).
10. Harvinder S. Gill., and Mark R. Prausnitz, Coated microneedles for transdermal delivery, Journal of Contrrol Release, 117(2), 227-237 (2007).
11. Mark R. Prausnitz, Microneedles for transdermal drug delivery Advanced Drug Delivery Reviews, 56(5), 581-587 (2004).
12. Jeong W. Lee, Jung-Hwan Park and Mark R. Prausnitz, Dissolving microneedles for transdermal drug delivery Biomaterials, 29(13), 2113-2124, (2008).
13. Jung-Hwan Park, Mark G. Allen and Mark R. Prausnitz. Biodegradable polymer microneedles: Fabrication, mechanics and transdermal drug delivery, Journal of Controlled Release, Volume 104(1), 5: 51-66, (2005).
14. Suzanne M. Bal, Julia Caussin, Stan Pavel and Joke A. Bouwstra, *In vivo* assessment of safety of microneedle arrays in human skin European Journal of Pharmaceutical Sciences, 35(3): 193-202 (2008).
15. F.J. Verbaan, S.M. Bal, D.J. van den Berg, Lüttge, Assembled microneedle arrays enhance the transport of compounds varying over a large range of molecular weight across human dermatomed skin Journal of Controlled Release, Volume 117(2): 238-245, (2007).
16. Ampere A. Tseng, Ying-Tung Chen, Choung-Lii Chao, Optics and Lasers in Engineering, Volume 45, Issue 10, pp. 975-992, (2007).